Article

Field continuous measurement of dissolved gases with a CF-MIMS: Applications to the physics and biogeochemistry of groundwater flow

Eliot Chatton, Thierry Labasque, Jérôme de La Bernardie, Nicolas Guihéneuf, Olivier Bour, and Luc Aquilina

Just Accepted

Field continuous measurement of dissolved gases with a CF-MIMS: Applications to the physics and biogeochemistry of groundwater flow

Authors: Eliot Chatton [a,*], Thierry Labasque [a], Jérôme de La Bernardie [a], Nicolas Guihéneuf [a,b], Olivier Bour [a], Luc Aquilina [a]

* Corresponding author.

[a] Géosciences Rennes, Université de Rennes 1-CNRS, UMR 6118, adress: 263 avenue du général Leclerc, Campus de Beaulieu, bâtiment 15, 35042 Rennes Cedex, France, phone: (+33) 223 233 725, email: eliot.chatton@gmail.com, thierry.labasque@univ-rennes1.fr, jerome.delabernardie@univ-rennes1.fr, olivier.bour@univ-rennes1.fr, luc.aquilina@univ-rennes1.fr.

[b] University of Guelph, 50 Stone Road East Guelph, Ontario, Canada, email: guiheneuf.nicolas@gmail.com

Keywords: *Dissolved gases*, *Noble gases*, *Groundwater*, *Tracer test*, *Noble Gas Temperature*, *Residence time*, *biogeochemical reactivity*, *MIMS*.

1   **Abstract**

2   In the perspective of a temporal and spatial exploration of aquatic environments (surface and ground

3   water), we developed a technique for field continuous measurements of dissolved gases with a precision

4   better than 1% for N_2, O_2, CO_2, He, Ar, 2% for Kr, 8% for Xe, and 3% for CH_4, N_2O and Ne. With a large

5   resolution (from 1×10^{-9} to 1×10^{-2} ccSTP/g) and a capability of high frequency analysis (1 measure every 2

6   seconds), the CF-MIMS (Continuous Flow Membrane Inlet Mass Spectrometer) is an innovative tool

7   allowing the investigation of a large panel of hydrological and biogeochemical processes in aquatic

8   systems.

9   Based on the available MIMS technology, this study introduces the development of the CF-MIMS

10   (conception for field experiments, membrane choices, ionisation) and an original calibration procedure

11   allowing the quantification of mass spectral overlaps and temperature effects on membrane permeability.

12   This study also presents two field applications of the CF-MIMS involving the well-logging of dissolved

13   gases and the implementation of groundwater tracer tests with dissolved ^{4}He. The results demonstrate the

14   analytical capabilities of the CF-MIMS in the field. Therefore, the CF-MIMS is a valuable tool for the

15   field characterisation of biogeochemical reactivity, aquifer transport properties, groundwater recharge,

16   groundwater residence time and aquifer-river exchanges from few hours to several weeks experiments.

17
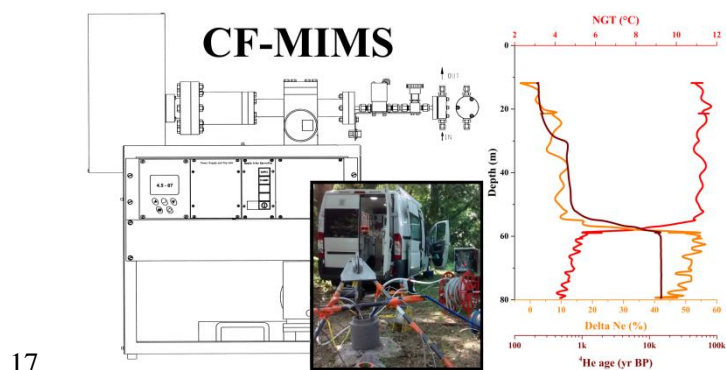
Introduction

19   Dissolved gas concentrations in groundwater originate mainly from atmosphere-water equilibria existing

20   at the water table during aquifer recharge. These equilibria are governed by physical laws allowing the

21   calculation of dissolved gas equilibrium concentrations (solubilities) as a function of the gas partial

22   pressure in the air (z_i), the atmospheric pressure (P), the water temperature (T) and salinity (S) [1–8].

23   Therefore, the combined determination of any dissolved gas concentration unaltered from recharge

24   equilibrium enables the reconstruction of recharge conditions (T, S, P) as long as the gas partial pressures

25   at the time of recharge are known. Consequently, several studies have been using dissolved noble gases [9–

26   11] sometimes combined to dissolved nitrogen [12,13] to derive past and present climatic conditions through

27   the determination of noble gas temperatures (NGTs i.e. recharge temperatures), the extent of the excess air

28   phenomenon (EA) and recharge elevations. Therefore, dissolved noble gases (and dissolved nitrogen) are

29   valuable tools for the study of groundwater origins, paleoclimates and climate changes.

30   Contrary to other noble gases, dissolved ^{4}He concentrations in groundwater can increase quite rapidly

31   (over a hundred years) due to *in situ* production by radioactive decay of uranium and thorium rich

32   minerals of aquifer rocks. As a result, dissolved radiogenic ^{4}He accumulates over time in aquifers and its

33   production creates an excess He that can be typically quantified for residence time larger than hundred

34   years. The determination of dissolved radiogenic He concentrations enables the characterisation of

35   groundwater residence times as long as ^{4}He production rates are known [14–17].

36   Dissolved reactive gases (N_2, CO_2, O_2, CH_4, N_2O and H_2) originate initially from atmospheric equilibria.

37   However, their concentrations in natural waters can be significantly altered by biogeochemical reactions

38   that typically occur in aquatic environments [18]. Therefore, the measurement of these reactive dissolved

39   gases is critical to the understanding of the biogeochemical reactivity of aquatic environments [19–25].

40   All these applications need precise dissolved gas measurements with various requirements in terms of

41   spatial and temporal distribution in the field. Currently, most of the available analytical techniques are

42   based on field sampling and laboratory analysis performed from a few hours or several days after

43   sampling. Therefore, ensuring sample preservation and representativeness is crucial for the determination

44   of accurate actual dissolved gas concentrations. For instance, groundwater sampling in wells is not an easy

45   task due to the risk of sample contamination with atmospheric air, the mixing processes naturally

46   occurring in the well (natural flows) or induced by the sampling process (renewal of the well water,

47   pumping, movement of mobile samplers) that would bias water samples [26]. Furthermore, preservation of

48   dissolved gas samples is a crucial stake particularly for the measurement of dissolved reactive gases such

49   as O_2, N_2, N_2O and H_2 in reactive environments.

50 In order to solve the issues related to sampling, field measurement techniques such as Membrane Inlet

51 Mass Spectrometers (MIMS) received great attention from environmental scientists for their capacity of

52 rapid evaluation of dissolved gases in water [27–32]. MIMS technology was first developed for the

53 measurement of organic compounds in environmental water samples [33,34]. Later, Ketola et al [35] proposed a

54 review of the applications and improvements of this technique. Kana et al [36] optimised a MIMS for quasi-

55 continuous determination of major dissolved gases (O_2, N_2, Ar) in water samples in order to study

56 biological activity [37–40]. MIMS systems were also miniaturised for oceanographic studies in order to create

57 dissolved gas profiles in seawater [41–44]. Recently, developments of MIMS have been realised for

58 groundwater studies. Mächler et al [45] developed a portable GE-MIMS for field and laboratory

59 measurements. This stand-alone system allows the quasi-continuous monitoring of dissolved He, Ar, Kr,

60 N_2 and O_2 every 12 minutes over several days. Similarly, Visser et al [46] developed also their own portable

61 NG-MIMS for quasi-continuous measurements of the whole suite of dissolved noble gases. However, the

62 NG-MIMS remains sensitive to the sampling conditions as it requires the collection of water samples that

63 are sequentially analysed (every 5 minutes). Furthermore, the available field quasi-continuous techniques

64 (GE-MIMS and NG-MIMS) do not allow so far the measurement of all major dissolved gases.

65 We propose here a new approach for the continuous field measurement of dissolved gases in aquatic

66 environments with a CF-MIMS (Continuous Flow Membrane Inlet Mass Spectrometer). Through this

67 technique, natural waters (surface water or groundwater) are directly brought to a semi-permeable

68 membrane at a constant flow rate for the continuous measurement of dissolved gases. With an original

69 calibration procedure, the CF-MIMS allows the continuous monitoring of dissolved noble and reactive

70 gases (He, Ne, Ar, Kr, Xe, N_2, CO_2, O_2, CH_4 and N_2O) over a large concentration range. After presenting

71 the details of the analytical development, the capabilities of the CF-MIMS are evaluated through two field

72 applications: two groundwater tracer tests with dissolved [4]He and a well-logging of dissolved gases.

Method

System description

Many MIMS systems are currently available on the market for different applications. The design and conception of the CF-MIMS (HPR-40) was carried out by the private supplier Hiden Analytical. According to the specification requirements, the instrument dimensions (0.150 m^3), weight (55 kg) and shielding (reinforced frame mounted on Silent Bloc®) make the CF-MIMS a mobile and resistant tool designed for field experiments.
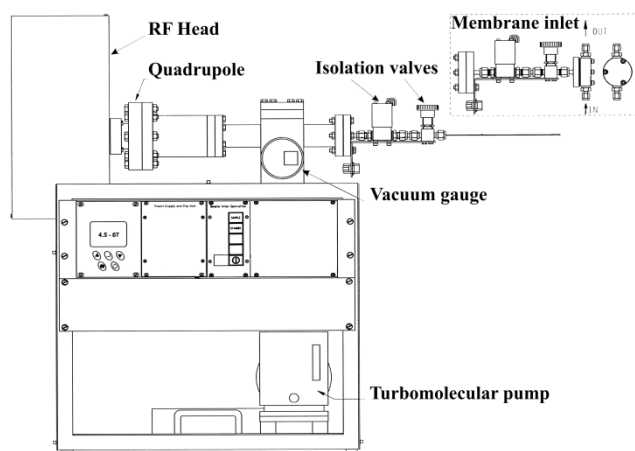
Figure 1: Representation of the CF-MIMS adapted from Hiden Analytical HPR40 manual.

Although its robustness, the CF-MIMS consists in a leading-edge analytical instrument for dissolved gas measurements. Equipped with a membrane inlet connected to the vacuum of a Quadrupole Mass Spectrometer (QMS around 10^{-5} Torr), the CF-MIMS shown in figure 1 allow the direct permeation of dissolved gases from liquids to the mass spectrometer. Inside the QMS, dissolved gases are ionised using an oxide coated iridium filament allowing the selection of ionisation energies (between 4 and 150 eV) and emission intensities (between 20 and 5000 µA). Once ionised, dissolved gases are separated by the quadrupole according to their mass to charge ratios (m/z ratios). Then, the detection of dissolved gases is performed either by a Faraday cup or a single channel electron multiplier (SCEM). Finally, the CF-MIMS

90   allows a direct and continuous measurement of dissolved gases at the high frequency of 1 dissolved gas

91   measurement every 2 seconds.

Optimisation techniques

92

Membrane

93

94   The originality of MIMS systems lies in the inlet that uses a semi-permeable membrane to measure

95   directly the dissolved gases of the water. The choice of a suitable membrane is therefore essential to

96   ensure the maximal permeation of the targeted dissolved gases. Laboratory experiments have been carried

97   out at Hiden Analytical to select or create the best membrane for our purposes by comparing different

98   types of membrane (PDMS, Biaxially oriented PET, X44® polymer). With an enhanced noble gas

99   permeability and a suitable gas exchange surface (16 cm²), the membrane X44® has been selected for our

100 CF-MIMS. This membrane inlet system (figure 1) allows a continuous flow measurement of dissolved

101 gases.

Water vapour entrapment

102

103 In order to enhance the sensitivity of MIMS systems to low abundant gases a water trap can be installed

104 just between the membrane inlet and the mass spectrometer [46]. However, the water trap requires a long

105 stabilisation time to remove the totality of the water vapour from the signal and uses lots of electrical

106 power that is hardly available in the field. Since this water entrapment did not significantly enhance

107 signal/noise ratios in our CF-MIMS we chose not to use it.

Ionisation

108

109 Inside the mass spectrometer, optimisation of ionisation procedures can be performed to improve the

110 signal/noise ratio by optimisation of the emission intensity (flow of ionising electrons) or, to a lower

111 extent, by experimental determination of optimal ionisation energies. In the CF-MIMS, the standard

112 ionisation procedure (250 µA, 70 eV) has been optimised by increasing the emission intensity in order to

113 enhance the sensitivity to low abundant gases such as Kr and Xe (see Supporting Information).

Calibration

In order to convert the partial pressures measured by the CF-MIMS into gas concentrations it is necessary to define a proper calibration procedure. In order to account for the different membrane interactions with dissolved gas concentrations, the system is directly calibrated on water flows of known concentration. For the purpose, a calibration chamber has been built in order to saturate a water volume with different standard gas mixtures of known composition while preventing from any atmospheric exchange (see Supporting Information). The Standard Gas Equilibrated Water (SGEW) is continuously brought from the calibration chamber to the membrane using a low voltage impeller pump allowing the monitoring of water saturation until equilibrium is reached.

Measured partial pressures for each gas can be converted into gas concentrations using either an internal or external calibration procedure. The internal calibration consists in the calculation of dissolved gas equilibrium concentrations of different SGEWs using the laws of gas solubility in water [1–8]. The parameters required for the calculation of equilibrium concentrations such as air pressure, water temperature and salinity are continuously monitored in the calibration chamber. In addition, the calibration chamber includes an outlet valve allowing an external calibration by sampling each SGEW for control analysis using classical gas-chromatography techniques (GC-TCD or GC-MS).

The calibration procedure is performed after connecting the membrane inlet to the mass spectrometer and should be implemented when the partial pressure baselines are stable (requiring almost 2 hours to establish an equilibrium between the permeation of gases through the membrane and the mass spectrometer vacuum). Calibration temporal stability has been investigated through a laboratory test that did not indicate any sign of instrumental drift over the 38 hours experiment. Therefore, when the calibration is achieved and as long as the membrane inlet remains connected, the CF-MIMS does not require any additional calibration. Nevertheless, regular sampling (for analysis with classical techniques) always ensures the validity of the calibration for long-term monitoring experiments.

138   The CF-MIMS calibration is performed at the same flow and temperature as the measurements because

139   membrane permeability to dissolved gases depends on water temperature and flow. Water flow is

140   controlled by an impeller/submersible pump serving the membrane (Q: 4L/min). Calibrations and

141   measurements are performed in a mobile laboratory conditioned at a controlled temperature close to the

142   temperature of the monitored water. However, when natural waters (in a river or in a borehole) show

143   temperature variations while monitoring, the signals measured with the CF-MIMS must be corrected from

144   temperature effects on the membrane permeability.

145   **Temperature sensitivity**

146   Laboratory experiments have been carried out to determine the influence of the water temperature on the

147   permeability of the membrane X44[®]. The results (see Supporting Information) show that the membrane

148   permeability to gases increases substantially with temperature. Small temperature variations ($\Delta T \pm 2°C$)

149   can modify the signal acquired at 17°C from 2.5% to 11.0% depending on the gas considered (He is less

150   sensitive than H_2O to temperature variations). However, the fitted curves allow the calculation of effective

151   permeability coefficients β_T^i of the gas i at the temperature T of measurement expressed in equation (1) as

152   the ratio of the partial pressure of the gas i at the temperature T on the partial pressure of the same gas i at

153   the temperature of calibration (T_{calib}).

154    $$\beta_T^i = \frac{P_T^i}{P_{Tcalib}^i} \quad (1)$$

155   The effective permeability coefficients are used when post-processing the data to correct temperature

156   effects on the membrane permeability for the different gases measured with the CF-MIMS.

157   **Spectral Overlaps**

158   In MIMS systems, the simplest case consists in measuring dissolved gases directly at their corresponding

159   m/z. For instance, the partial pressures of He, Ar, Kr, Xe and O_2 can be respectively associated to the m/z

160 at 4, 40, 84, 132 and 32. However, in mass spectrometry, spectral overlaps are issues frequently

161 encountered.

162 The objective of the CF-MIMS is to measure the full suite of noble gases (He, Ne, Ar, Kr, Xe) as well as

163 the most common dissolved gases (N_2, O_2, CO_2, CH_4 and N_2O). These dissolved species coexist in natural

164 waters and unfortunately some of them occur at m/z ratio overlapping with other gases as shown in table

165 1. Most of the time, the overlapping gases are also among the targeted ones which inhibits the use of traps

166 and getters [46] to remove the overlapping N_2, CO_2, CH_4, N_2O and Ar.

167 **Table 1: Spectral overlaps occurring at measured mass-to-charge ratios.**

m/z	Targeted gas	Main overlap	Second overlap
12	CO_2	CH_4	-
14	N_2	N_2O	-
15	CH_4	N_2	-
20	Ne	Ar	H_2O
22	Ne	CO_2	N_2O
28	N_2	N_2O	CO_2
44	CO_2/N_2O	-	-

168

169 Without traps and getters, the other way to remove overlapping species at a particular m/z ratio is to

170 optimise ionisation energies. For instance, laboratory tests have been carried out to distinguish Ne signals

171 from $^{20}(Ar_{(II)})$ and $^{20}(H_2O)$ or from $^{22}(CO_{2(II)})$ and $^{22}(N_2O_{(II)})$ using lower ionisation energies to avoid the

172 second ionisation of overlapping gases at m/z 20 and 22 respectively. Although ^{20}Ne and $^{20}(Ar_{(II)})$ could be

173 separated from $^{20}(H_2O)$, the attempts to fully discriminate (with ionisation energies) Ne signals from

174 $^{20}(Ar_{(II)})$, $^{22}(CO_{2(II)})$ or $^{22}(N_2O_{(II)})$ were unsuccessful despite the information reported in other works on

175 similar QMS systems [47,48].

176 Therefore, we choose to overcome the issue of spectral overlaps by calibrating the CF-MIMS with a

177 variety of suitable standard gases allowing the quantification of these overlaps. The idea here is to

178 quantify the distribution of a given gas on the different m/z ratios of interest. For instance, CO_2 is found at

179   m/z 12, 22, 28 and 44 (table 1) and its distribution over each of these m/z ratios can be measured and

180   expressed as polynomials (see Supporting Information). This is performed by monitoring the partial

181   pressures at these m/z ratios when saturating a volume of water in the calibration chamber with pure CO_2

182   and desaturating it with another pure gas (N_2, Ar, He, etc.). The same rationale applies for N_2 at m/z 14,

183   15, 28 and for Ar at m/z 20 and 40. The polynomials linking the partial pressures P_k^i and P_l^i of the gas i

184   measured respectively at m/z k and l are expressed in equation 2:

185    $$P_k^i = f\left(P_l^i\right) = \sum_{n=0}^{N} \alpha_n \left(P_l^i\right)^n \quad (2)$$

186   Once fitted to the data, the resulting polynomials allow the determination of relationships between each

187   m/z ratios due to each gas (CO_2, N_2 and Ar) over a large concentration range. As a result, any significant

188   partial pressure change away from the fitted polynomials indicates an overlap attributable either to Ne,

189   N_2O or CH_4 depending on the considered m/z. In this case, the partial pressure (P_k^j) attributed to the

190   overlapping gas j can be calculated as the difference between the total partial pressure (P_k) measured at

191   m/z k and the partial pressure (P_k^i) of the gas i at m/z k as expressed in equation 3:

192    $$P_k^j = P_k - P_k^i = P_k - \sum_{n=0}^{N} \alpha_n \left(P_l^i\right)^n \quad (3)$$

193   This method relies on multiple measurements at different m/z ratios of the same targeted gas to guarantee

194   a better precision (the gas is measured twice or thrice) and a better confidence respect to overlaps (the

195   different m/z ratios of a gas usually do not undergo the same overlap).

196   After calibration and measurement, the data files provided by the CF-MIMS are post-processed using a

197   data processing program implemented in Matlab® that calculates the partial pressure $P_{m/z}^i$ of the gas i at

198   m/z using the spectral overlap polynomials and the effective permeability coefficients β_T following

199   equation 4:

200    $$P_{m/z}^i = \beta_T^i * \left[P_{m/z} - \sum_j \left(\beta_T^j * \sum_{n=0}^{N} \alpha_n \left(P_{m/z}^j\right)^n\right)\right] \quad (4)$$

201　Dissolved gases undergoing overlaps are hence calculated as the difference between the measured partial

202　pressure at a given m/z and the sum of partial pressures produced by the overlapping species j weighted by

203　their effective permeability coefficients (β_T^j). Therefore, it is essential to properly assess the different

204　overlap polynomials.

205　Finally, the data processing program calculates and compiles the partial pressures of each gas free from

206　overlaps, determines internal or external calibration coefficients for each gas and provides the dissolved

207　gas concentrations that are delivered as a spreadsheet.

Analytical performances

209　For each dissolved gas, laboratory experiments have been carried out to evaluate the analytical precisions

210　of the CF-MIMS (expressed as the relative standard deviation, RSD) and the detection limits (DL) for

211　reactive (N_2, O_2, CO_2, CH_4, N_2O) and noble (He, Ne, Ar, Kr, Xe) gases. Table 2 shows the details of the

212　analytical performances of the CF-MIMS measured from three series of monitoring (2 hours) of an AEW

213　kept at a constant temperature (17°C). The analytical frequency of the instrument allows the measurement

214　of a m/z ratio every two seconds (the measurement of gas can require more than one m/z measurement).

215　Therefore, a measurement cycle of the 10 gases listed in the table 2 takes about 26 seconds.

216　**Table 2: Experimental assessment of the CF-MIMS gas measurement precisions (RSD) and estimated detection limits**

217　**(DL). Asterisks refer to DL estimations performed on the basis of 3×RSD of the most abundant gas at the measured m/z**

218　**for typical concentrations obtained with an AEW (CO_2= 4.3×10-4 ccSTP/g; N_2= 1.4×10^{-2} ccSTP/g).**

Gas	RSD (%)	DL ($\times 10^{-9}$ ccSTP/g)
N_2	0.3	750
O_2	0.3	2
CO_2	0.3	2000
CH_4	2.0	800*
N_2O	0.3	900*
He	1.0	0.01
Ne	2.5	6*
Ar	0.3	200
Kr	1.2	0.5

Xe	7.5	4

219 As Ne, CH_4 and N_2O are measured at overlapped m/z ratios, their detection limits depend also on the

220 analytical uncertainty of the main overlapping gas at these m/z ratios (respectively [22](CO_2), [15](N_2) and

221 [44](CO_2)). Table 2 displays an example of the detection limits calculated for Ne, CH_4 and N_2O for an air

222 equilibrated water ($[CO_2]_{atm}$=0.04% and $[N_2]_{atm}$=78.08%) expressed as three RSD of the main overlapping

223 gas. As a result, higher levels of N_2 or CO_2 would increase proportionally the detection limits of Ne, CH_4

224 and N_2O.

Field Applications

Groundwater tracer test with dissolved [4]He

227 In hydrogeology, groundwater introduced tracer tests are usually performed with salts or fluorescent dyes

228 in order to derive the transport properties of aquifers [49–51]. Although little used so far in tracer tests,

229 dissolved noble gases are inert tracers of the physical processes governing conservative transport in

230 aquifers such as advection, dispersion and diffusion [52–55]. Where classical tracers may possibly entail flaws

231 such as toxicity, sorption, degradation or density effects [56–58], dissolved noble gases can represent a

232 valuable alternative especially when implementing tracer tests in drinking water supply areas [59]. As a

233 result, we decided to evaluate the potential of the CF-MIMS to perform continuous and field

234 measurements through a groundwater tracer test using dissolved [4]He.

235 The groundwater tracer test was carried out in a fractured aquifer located at the experimental site of

236 Ploemeur (H+ observatory network, Brittany, France) at the contact zone between a granitic formation and

237 the overlying micaschist [60]. This vertical tracer test was performed in a single well (B3) and consisted in

238 the combined pulse injection of dissolved [4]He (60 L of He saturated water) and a fluorescent dye called

239 amino-G acid (7-Amino-1,3-naphthalenedisulfonic acid) in a fracture crossing the borehole at 44.9m

240 (B3.2) while pumping in an hydraulically connected fractured zone (B3.1) found in the same well at

241 34.0m. Tracer path was constrained into the fracture network using low flow injections (6 L/min) below a

242 single packer placed in the borehole between the two connected fractures.

243 Figure 2 shows the ^{4}He and amino-G acid (AG) breakthrough curves produced respectively by the CF-

244 MIMS and the fluorimeter over two tracer tests performed with two pumping rates (1.4 and 5.9 m^3/h). For

245 these short tracer tests, ^{4}He and AG show similar breakthrough curves (although ^{4}He systematically peaks

246 late) as well as similar fitted transport parameters (see Supporting Information) using a semi analytical

247 solution developed by Becker and Charbeneau [49]. For longer tracer tests, the differences between the two

248 breakthrough curves are expected to increase with time due to a higher He diffusion.
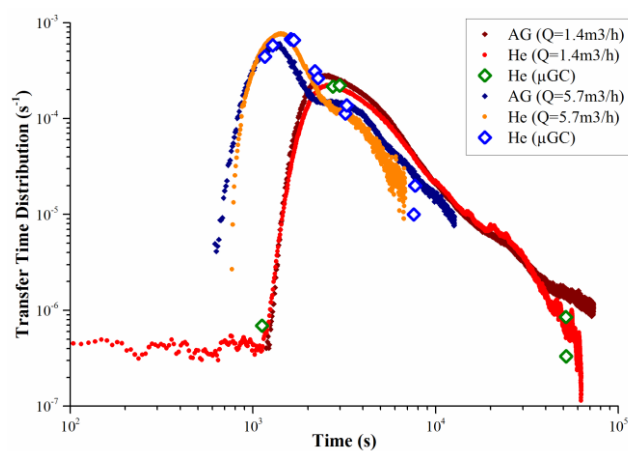
249

250 **Figure 2: ^{4}He and AG acid breakthrough curves obtained with two different pumping conditions (1.4 and 5.9 m^3/h). The**

251 **transfer time distribution curves (s^{-1}) refer to the tracer mass flux (g/s) divided by the recovered mass of tracer (g).**

252 This groundwater tracer tests show that the CF-MIMS is able to measure dissolved gas concentrations *in*

253 *situ* over experiments of several hours and to record ~~instantaneously~~ large concentration gradients with

254 high temporal resolution. The CF-MIMS measurements are directly validated by control sampling

255 performed during the two tracer tests and indirectly by AG breakthrough curves produced by the

256 fluorimeter.

Well-logging of dissolved gases

Classically, a first order characterisation of groundwater geochemistry is achieved using a multi-parameter probe allowing the vertical measurement of the field parameters in wells (temperature, electrical conductivity, pH, redox potential and dissolved oxygen). More detailed investigations require additional measurements that are usually performed through the sampling of targeted dissolved species (gases, ions, stable isotopes, etc.). The results of such geochemical characterisation are hardly available on the field and rely inherently on substantial uncertainties associated to sampling (representativeness, contamination and preservation of the sample). Besides, due to practical constrains the exhaustiveness (number of measured parameters, spatial and temporal distribution) of classical geochemical characterisation is often limited in view of the variety and variability of biogeochemical processes in time and space.

In order to test the method developed here, we have investigated the potential of performing a well-log of dissolved gases with the CF-MIMS in a borehole (Pz6) drilled in a schist bedrock and located nearby our laboratory in Rennes (H+ observatory, Brittany, France). The transportation and power supply of the CF-MIMS has been made possible thanks to the mobile laboratory arranged in an all-terrain truck (CRITEX Lab). This simple experiment consisted in coupling a multi-parameter probe (OTT® Hydrolab) to the well-pump (Grundfos® MP1) serving the CF-MIMS in order to measure the evolution with depth of dissolved gases concentrations (He, Ne, Ar, Kr, Xe, N_2, O_2, CO_2, CH_4), temperature (T), pH, electrical conductivity (σ) and redox potential (Eh). The pumping rate (3 L/min) and the logging velocity (2.5 m/min) have been adjusted to the borehole diameter, the number of measured dissolved gases and hence to the measurement frequency of the CF-MIMS (12 m/z every 24 s for 1 measure every meter).

The figure 3 shows the profiles that were obtained at Pz6 for the field parameters (figure 3a), the reactive dissolved gases (figure 3b) and the dissolved noble gases (figure 3c). This well-log consists in two contrasted groundwater bodies and two transition zones: (80-60m) high pH and conductivity, high reactive and noble gas concentrations except CO_2 and low Eh and O_2; (60-55m) a mixing zone where almost all the parameters change; (55-30m) lower pH, conductivity and dissolved gas concentrations except CO_2 that

282   increases, low O_2 and higher Eh. The shallowest part of the well (30-12m) shows a transition towards an

283   atmospheric dissolved gas composition.
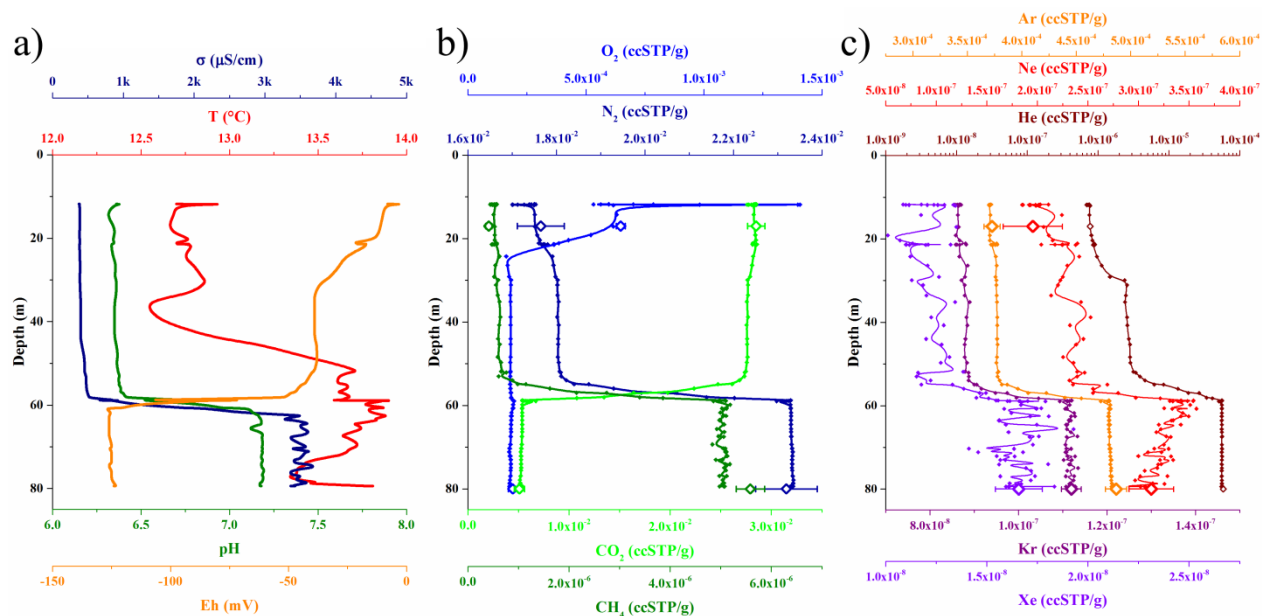
284

285   **Figure 3: Well-logs performed at Pz6 for (a) water temperature (T), electrical conductivity (σ), pH and redox potential**

286   **(Eh); (b) reactive dissolved gases (N_2, O_2, CO_2, CH_4); (c) dissolved noble gases (He, Ne, Ar, Kr, Xe). The large dots in b)**

287   **and c) refer to samples collected at 17m and 80m. Continuous lines refer to a spline fit of the data points shown as small**

288   **dots in the figure.**

289   During the well-logging experiment discrete samples were collected and analysed using accepted

290   analytical protocols [46,61,62]. A comparison of these analyses with the CF-MIMS measurements is shown in

291   table 3. Both measurements agree for all dissolved gases analysed within the error of the respective

292   methods.

293   **Table 3: Comparison of CF-MIMS measurements with measurements of dissolved gases in Pz6 conducted either (*) at the**

294   **University of Rennes by gas-chromatography [61,62] or (#) in situ by mass-spectrometry with a NG-MIMS [46].**

Depth (m)	Gas*#	Sample (ccSTP/g)	Sample RSD (%)	CF-MIMS (ccSTP/g)	CF-MIMS RSD (%)	Relative difference (%)
	N_2*	1.76×10^{-2}	3.0	1.75×10^{-2}	0.3	0.5
17	O_2*	6.48×10^{-4}	3.0	6.21×10^{-4}	1.3	3.0
	CO_2*	2.85×10^{-2}	3.0	2.84×10^{-2}	0.3	0.5

	CH$_4$*	4.11×10^{-7}	15.0	5.29×10^{-7}	3.0	17.5
	He*	7.75×10^{-7}	3.0	1.19×10^{-6}	3.5	1.0
	Ne*	1.96×10^{-7}	10.0	2.11×10^{-7}	5.0	5.5
	Ar*	3.73×10^{-4}	2.5	3.71×10^{-4}	0.1	0.5
80	N$_2$*	2.32×10^{-2}	3.0	2.33×10^{-2}	0.1	0.5
	O$_2$*	1.90×10^{-4}	10.0	1.77×10^{-4}	0.6	5.0
	CO$_2$*	5.09×10^{-3}	10.0	5.24×10^{-3}	2.1	2.0
	CH$_4$*	5.59×10^{-6}	5.0	5.05×10^{-6}	0.7	7.0
	He$^{\#}$	5.88×10^{-5}	2.0	5.82×10^{-5}	1.3	3.0
	Ne$^{\#}$	3.13×10^{-7}	6.5	3.04×10^{-7}	4.8	2.0
	Ar$^{\#}$	4.87×10^{-4}	2.0	4.83×10^{-4}	0.1	0.5
	Kr$^{\#}$	1.12×10^{-7}	2.0	1.12×10^{-7}	0.7	0.5
	Xe$^{\#}$	1.66×10^{-8}	6.5	1.66×10^{-8}	5.2	0.5

295

296   The field measurement of dissolved noble gas concentrations allow to derive profiles of groundwater

297   recharge conditions [63] and the amount of non-atmospheric ^{4}He produced by radiogenic U and Th of the

298   rocks. With no mantle He and using a production rate of 4×10^{-9} ccSTP/g/yr for ^{4}He calibrated on ^{14}C ages

299   [64], the groundwater residence time can be assessed for regional groundwater circulations using ^{4}He dating

300   [17]. Figure 4 shows the field determination of the distribution with depth of noble gas temperatures (NGTs

301   i.e. recharge temperatures), amounts of excess air (commonly expressed as the $\Delta Ne = ((CNe_{meas}/CNe_{eq})-$

302   $1)\times100)$ and ^{4}He ages.
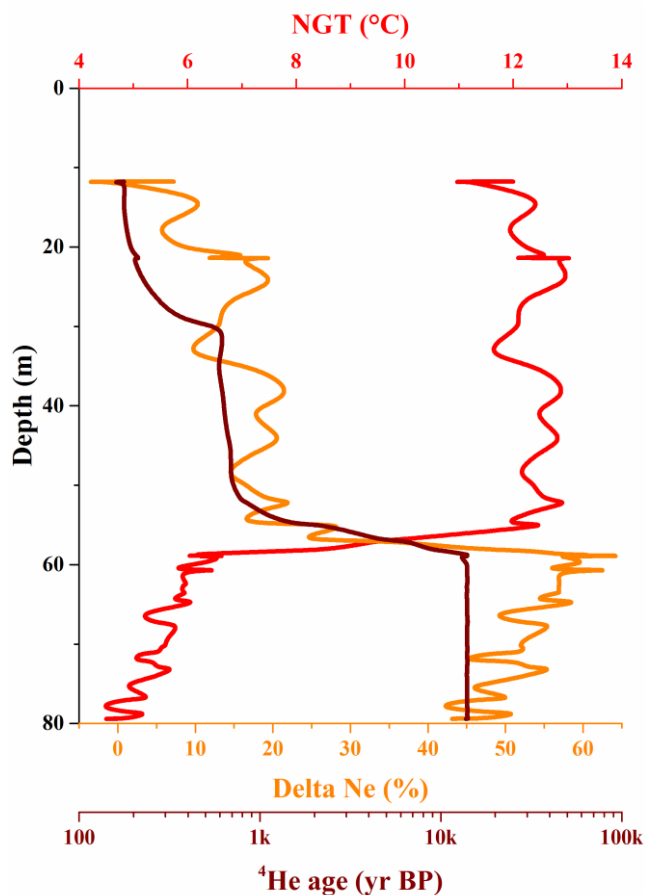
303

304   **Figure 4: Profile of noble gas temperature (NGT), ΔNe and ^{4}He age distribution with depth.**

305   Similarly to the previous profiles, the figure 4 shows three groundwater layers: (80-60m) low NGTs (≈

306   5°C) associated with large ΔNe (≈ 50%) and ^{4}He ages (≈ 14,000 yr BP); (60-55m) mixing zone; (55-12m)

307   NGTs around 11°C associated with smaller ΔNe (≈ 10%) and ^{4}He ages (≈ 500 yr BP). The shallowest part

308   of this layer (30-12m) shows decreasing ΔNe (0% in average) and ^{4}He ages (≈ 200 yr BP) towards the

309   water table.

310   This field experiment illustrates the usefulness of field measurements of dissolved gases for the

311   characterisation of groundwater chemistry and the determination of groundwater origins. The field

312   continuous measurements performed with the CF-MIMS make available a quantity of valuable distributed

313   information so far inaccessible during field works.

Discussion

Calibration

Precise dissolved gas measurements with a CF-MIMS can only be achieved with a proper calibration procedure which is not so trivially accomplished because it is performed on SGEWs (a precise determination of their composition is essential) with a water flow and temperature dependent membrane permeability (a precise determination of these effects is also necessary). In addition, calibration of Ne, CH_4 and N_2O require a special care (use of additional SGEWs) in order to overcome spectral overlap issues.

When the calibration procedure is properly achieved and as long as the membrane inlet remains connected to the mass spectrometer, the CF-MIMS allow a continuous monitoring of dissolved gases over relatively long experiments (days or weeks) without additional calibration (standard bracketing). The latter would alter the benefits of the continuous measurements since the CF-MIMS measurements require as much stability as possible. For long monitoring experiments we thus recommend a regular sampling to ensure the validity of the calibration. So far, biogeochemical clogging of the membrane has not been observed which might be explained by the nature of the membrane X44®.

Capabilities of the CF-MIMS

First, the dissolved gas tracer tests demonstrate the ability of the CF-MIMS to perform field dissolved gas measurements accurate enough to produce appropriate breakthrough curves during groundwater tracer tests. This experiment exhibits the instrument capabilities for high-frequency measurements and its rapidity to quantify large concentration gradients. The CF-MIMS offer new perspectives for groundwater tracer tests enabling the use of new tracers (noble and reactive gases) and allowing a combined injection of several tracers of different nature (salts, fluorescent tracers, dissolved gases, etc.).

336   As for tracer tests, the well-logging experiment demonstrates the ability of the CF-MIMS to work at high-

337   frequency *in situ* and provide accurate environmental measurements allowing in this case the

338   determination of groundwater recharge conditions, groundwater residence time and redox conditions

339   profiles. These field continuous measurements do not only solve the problems associated to sampling

340   (representativeness, contamination or preservation of samples) but also, taken as a whole, improve the

341   quality of the information carried by each value of the dataset (enhanced representativeness with

342   distributed measurements and enhanced precision with several replicates). Therefore, the CF-MIMS gives

343   access to spatially and temporally distributed data of great significance that represents an important

344   breakthrough for environmental measurements.

345   In addition, the CF-MIMS ability to produce field continuous measurements allows the scientist to

346   visualise and interpret the data directly on site allowing a better definition of field experiment strategies

347   and a higher flexibility when implementing them. Finally, the rationale behind the CF-MIMS technology

348   consists in bringing back environmental scientists on the field to get a much more thorough understanding

349   of the site structure and properties all along the experiments.

350   **Potential Applications**

351   Once installed in the mobile laboratory, the CF-MIMS has the required mobility to perform *in situ*

352   measurements in a large diversity of accessible areas (boreholes, rivers, vadose zone, sea or lake shores,

353   wetlands). In these sites, the high-frequency and multi-tracer measurements offered by this instrument

354   allow the observation of a variety of stable to highly-transitory physical, chemical or biological

355   phenomena modifying dissolved gases concentrations (water flow, mixing, degassing, biochemical

356   consumption/production of one or more gas(es)). Therefore, the CF-MIMS is a valuable tool for the field

357   characterisation of biogeochemical reactivity in aquatic systems, aquifer and river transport properties,

358   groundwater recharge conditions, groundwater residence time (^{4}He, ^{40}Ar) and aquifer-river exchanges.

359   **Associated Contents**

360   **Supporting Information**

361   Measurement settings, Instrumental drift, Temperature Sensitivity, Calibration standard gases, Overlap

362   extents, Tracer test details, Part List. This material is available free of charge via the Internet at

363   http://pubs.acs.org.

373   **References**

(1)   Clever, H. L. Helium and Neon - Gas Solubilities. *Solubility data Ser*. **1979**, *1*, 393.

(2)   Clever, H. L. Krypton, Xenon and Radon - Gas-Solubilities. *Solubility data Ser*. **1979**, *2*, 357; doi:10.1016/0378-3812(80)80030-6.

(3)   Clever, H. L. Argon. *Solubility data Ser*. **1980**, *4*, 331; doi:10.1016/0021-9614(80)90193-7.

(4)   Smith, S. P.; Kennedy, B. M. The solubility of noble gases in water and in NaCl brine. *Geochim. Cosmochim. Acta* **1983**; *41*(1), 503-515.

(5)   Weiss, R. F. The solubility of nirogen, oxygen and argon in water and seawater. *Deep-Sea Res*.

1970, *17*, 721-735.

(6)   Weiss, R. F. Carbon dioxide in water and seawater: the solubility of a non-ideal gas. *Mar. Chem*.

1974, *2*, 203-215.

(7)   Weiss, R. F.; Price, B. A. Nitrous oxide solubility in water and seawater. *Mar. Chem*. **1980**, *8*, 347-

359; doi:10.1016/0304-4203(80)90024-9.

(8)   Wiesenburg, D. A.; Guinasso, N. L. Equilibrium solubilities of methane, carbon monoxide, and

hydrogen in water and sea water. *J. Chem. Eng. Data* **1979**, *24*(4), 356-360;

doi:10.1021/je60083a006.

(9)   Aeschbach-Hertig, W.; Peeters, F.; Beyerle, U.; Kipfer, R. Interpretation of dissolved atmospheric

noble gases in natural waters. *Water Resour. Res*. **1999**, *35*(9), 2779-2792.

(10)   Aquilina, L.; Vergnaud-Ayraud, V.; Armandine Les Landes, A.; Pauwels, H.; Davy, P.; Petelet-

Giraud, E.; Labasque, T.; Roques, C.; Chatton, E.; Bour, O.; Ben Maamar, S.; Dufresne, A.;

Khaska, M.; Le Gal La Salle, C.; Barbecot, F. Impact of climate changes during the last 5 million

years on groundwater in basement aquifers. *Sci. Rep*. **2015**, *5*, 14132; doi:10.1038/srep14132.

(11)   Stute, M.; Schlosser, P. Principles and applications of the noble gas paleothermometer. In

Geophysical Monograph Series, **1993**, *78*.

(12)   Chatton, E.; Aquilina, L.; Petelet-Giraud, E.; Cary, L.; Bertrand, G.; Labasque, T.; Hirata, R.;

Martins, V.; Montenegro, S.; Vergnaud, V.; Aurouet, A.; Kloppmann, W.; Pauwels, H. Glacial

recharge, salinization and anthropogenic contamination in the coastal aquifers of Recife (Brazil).

Sci. Total Environ. **2016**, *569-570*, 1114-1125; doi:10.1016/j.scitotenv.2016.06.180.

(13)   Plummer, L. N.; Eggleston, J. R.; Andreasen, D. C.; Raffensperger, J. P.; Hunt, A. G.; Casile, G. C.

Old groundwater in parts of the upper Patapsco aquifer, Atlantic Coastal Plain, Maryland, USA:

evidence from radiocarbon, chlorine-36 and helium-4. *Hydrogeol. J.* **2012**, *20*(7), 1269-1294; doi:10.1007/s10040-012-0871-1.

(14) Andrews, J. N.; Davis, S. N.; Fabryka-Martin, J.; Fontes, J. C.; Lehman, B. E.; Loosli, H. H.; Michelot, J. L.; Moser, H.; Smith, B.; Wolf, M. The in situ production of radioisotopes in rock matrices with particular reference to the Stripa granite. *Geochim. Cosmochim. Acta* **1989**, *53*, 1803-1815.

(15) Méjean, P.; Pinti, D. L.; Larocque, M.; Ghaleb, B.; Meyzonnat, G.; Gagné, S. Processes controlling 234U and 238U isotope fractionation and helium in the groundwater of the St. Lawrence Lowlands, Quebec: The potential role of natural rock fracturing. *Appl. Geochem.* **2016**, *66*, 198-209; doi:10.1016/j.apgeochem.2015.12.015.

(16) Solomon, D. K.; Hunt, A. G.; Poreda, R. J. Source of radiogenic helium 4 in shallow aquifers: Implications for dating young groundwater. *Water Resour. Res.* **1996**, *32*(6), 1805-1813; doi:10.1029/96WR00600.

(17) Wei, W.; Aeschbach-hertig, W.; Chen, Z. Identification of He sources and estimation of He ages in groundwater of the North China Plain. *Appl. Geochem.* **2015**, *63*, 182-189; doi:10.1016/j.apgeochem.2015.08.010.

(18) Boisson, A.; De Anna, P.; Bour, O.; Le Borgne, T.; Labasque, T.; Aquilina, L. Reaction chain modeling of denitrification reactions during a push-pull test. *J. Contam. Hydrol.* **2013**, *148*, 1-11; doi:10.1016/j.jconhyd.2013.02.006.

(19) Abbott, B. W.; Jones, J. B.; Godsey, S. E.; Larouche, J. R.; Bowden, W. B. Patterns and persistence of hydrologic carbon and nutrient export from collapsing upland permafrost. *Biogeosciences* **2015**, *12*(12), 3725-3740; doi:10.5194/bg-12-3725-2015.

(20) Beaulieu, J. J.; Tank, J. L.; Hamilton, S. K.; Wollheim, W. M.; Hall, R. O.; Mulholland, P. J.;

Peterson, B. J.; Ashkenas, L. R.; Cooper, L. W.; Dahm, C. N.; Dodds, W. K.; Grimm, N. B.; Johnson, S. L.; McDowell, W. H.; Poole, G. C.; Maurice Valett, H.; Arango, C. P.; Bernot, M. J.; Burgin, A. J.; Crenshaw, C. L.; Helton, A. M.; Johnson, L. T.; O'Brien, J. M.; Potter, J. D.; Sheibley, R. W.; Sobota, D. J.; Thomas, S. M. Nitrous oxide emission from denitrification in stream and river networks. *Proc. Natl. Acad. Sci. U.S.A.* **2011**, *108*(1), 214-219; doi:10.1073/pnas.1011464108.

(21) Gardner, J. R.; Fisher, T. R.; Jordan, T. E.; Knee, K. L. Balancing watershed nitrogen budgets: accounting for biogenic gases in streams. *Biogeochemistry*. **2016**, *127*(2-3), 231-253; doi:10.1007/s10533-015-0177-1.

(22) Kling, G. W.; Kipphut, G. W.; Miller, M. C. Arctic Lakes and Streams as Gas Conduits to the Atmosphere: Implications for the Tundra Carbon Budgets. *Science* **1991**, *251*(4991), 298-301.

(23) Mächler, L.; Brennwald, M. S.; Tyroller, L.; Livingstone, D. M.; Kipfer, R. Conquering the outdoors with on-site mass spectrometry. *Chimia* **2014**, *68*(3), 155-159; doi:10.2533/chimia.2014.155.

(24) Peter, S.; Mächler, L.; Kipfer, R.; Wehrli, B.; Durisch-Kaiser, E. Flood-Controlled Excess-Air Formation Favors Aerobic Respiration and Limits Denitrification Activity in Riparian Groundwater. *Front. Environ. Sci.* **2015**, *3*, 75; doi:10.3389/fenvs.2015.00075.

(25) Riley, A. J.; Dodds, W. K. Whole-stream metabolism: strategies for measuring and modeling diel trends of dissolved oxygen. *Freshw. Sci.* **2013**, *32*(1), 56-69; doi:10.1899/12-058.1.

(26) Reilly, T. E.; LeBlanc, D. R. Experimental Evaluation of Factors Affecting Temporal Variability of Water Samples Obtained from Long-Screened Wells. *Ground Water* **1998**, *36*(4), 566-576.

(27) Cowie, G.; Lloyd, D. Membrane inlet ion trap mass spectrometry for the direct measurement of dissolved gases in ecological samples. *J. Microbiol. Methods* **1999**, *35*(1), 1-12;

doi:10.1016/S0167-7012(98)00090-6.

(28) Kotiaho, T. On-site environmental and in situ process analysis by mass spectrometry. *J. Mass Spectrom*. **1996**, *31*(1), 1-15.

(29) Lloyd, D.; Scott, R. I. Direct measurement of dissolved gases in microbiological systems using membrane inlet mass spectrometry. *J. Microbiol. Methods* **1983**, *1*(6), 313-328; doi:10.1016/0167-7012(83)90008-8.

(30) Takahata, N.; Igarashi, G.; Sano, Y. Continuous monitoring of dissolved gas concentrations in groundwater using quadrupole mass spectrometer. *Appl. Geochem*. **1997**, *12*(4), 377-382.

(31) Virkki, V. T.; Ketola, R. A.; Ojala, M.; Kotiaho, T.; Komppa, V.; Grove, A.; Facchetti, S. On-Site Environmental Analysis by Membrane Inlet Mass Spectrometry. *Anal. Chem*. **1995**, *67*(8), 1421-1425; doi:10.1021/ac00104a019.

(32) White, A. J.; Blamire, M. G.; Corlett, C. A.; Griffiths, B. W.; Martin, D. M.; Spencer, S. B.; Mullock, S. J. Development of a portable time-of-flight mebrane inlet mass spectrometer for environmental analysis. *Rev. Sci. Instrum*. **1998**, *69*, 565; doi:10.1063/1.1148695.

(33) Hemond, H. F. A backpack-portable mass spectrometer for measurement of volatile compounds in the environment. *Rev. Sci. Instrum*. **1991**, *62*, 1420; doi:10.1063/1.1142461.

(34) Lauritsen, F. R.; Bohatka, S.; Degn, H. A Membrane-inlet Tandem Mass Spectrometer for Continuous Monitoring of Volatile Organic Compounds. *Rapid Commun. Mass Spectrom*. **1990**, *4*(10), 401-403.

(35) Ketola, R. A.; Kotiaho, T.; Cisper, M. E.; Allen, T. M. Environmental applications of membrane introduction mass spectrometry. *J. Mass Spectrom*. **2002**, *37*(5), 457-476; doi:10.1002/jms.327.

(36) Kana, T. M.; Darkangelo, C.; Hunt, M. D.; Oldham, J. B.; Bennett, G. E.; Cornwell, J. C.

Membrane inlet mass spectrometer for rapid high-precision determination of N2, O2, and Ar in environmental water samples. *Anal. Chem*. **1994**, *66*(23), 4166-4170; doi:10.1021/ac00095a009.

(37)   An, S.; Gardner, W. S.; Kana, T. M. Simultaneous Measurement of Denitrification and Nitrogen Fixation Using Isotope Pairing with Membrane Inlet Mass Spectrometry Analysis. *Appl. Environ. Microbiol*. **2001**, *67*(3), 1171-1178; doi:10.1128/AEM.67.3.1171.

(38)   Bohatka, S.; Futo, I.; Gal, I.; Gal, J.; Langer, G.; Molnar, J.; Paal, A.; Pinter, G.; Simon, M.; Szadai, J.; Szekely, G. Quadrupole mass spectrometer system for fermentation monitoring. *Vacuum* **1993**, *44*(5-7), 669-671; doi:10.1016/0042-207X(93)90121-P.

(39)   Degn, H. Membrane inlet mass spectrometry in pure and applied microbiology. *J. Microbiol. Methods* **1992**, *15*(3), 185-197; doi:10.1016/0167-7012(92)90039-7.

(40)   Eschenbach, W.; Well, R. Online measurement of denitrification rates in aquifer samples by an approach coupling an automated sampling and calibration unit to a membrane inlet mass spectrometry system. *Rapid Commun. Mass Spectrom*. **2011**, *25*(14), 1993-2006; doi:10.1002/rcm.5066.

(41)   Bell, R. J.; Short, R. T.; Van Amerom, F. H. W.; Byrne, R. H. Calibration of an in situ membrane inlet mass spectrometer for measurements of dissolved gases and volatile organics in seawater. *Environ. Sci. Technol*. **2007**, *41*(23), 8123-8128; doi:10.1021/es070905d.

(42)   Gentz, T.; Schlüter, M. Underwater cryotrap-membrane inlet system (CT-MIS) for improved in situ analysis of gases. *Limnol. Oceanogr. Methods* **2012**, *10*, 317-328; doi:10.4319/lom.2012.10.317.

(43)   Short, R. T.; Fries, D. D.; Kerr, M. L.; Lembke, C. E.; Toler, S. K.; Wenner, P. G.; Byrne, R. H. Underwater mass spectrometers for in-situ chemical analysis of the hydrosphere. *J. Am. Soc. Mass Spectrom*. **2001**, *12*(1); 676-682.

(44)   Tortell, P. D. Dissolved gas measurements in oceanic waters made by membrane inlet mass spectrometry. *Limnol. Oceanogr. Methods* **2005**, *3*, 24-37; doi:10.4319/lom.2005.3.24.

(45)   Mächler, L.; Brennwald, M. S.; Kipfer, R. Membrane Inlet Mass Spectrometer for the Quasi-Continuous On-Site Analysis of Dissolved Gases in Groundwater. *Environ. Sci. Technol*. **2012**, *46*, 8288-8296; doi:10.1021/es3004409.

(46)   Visser, A.; Singleton, M. J.; Hillegonds, D. J.; Velsko, C. A.; Moran, J. E.; Esser, B. K. A membrane inlet mass spectrometry system for noble gases at natural abundances in gas and water samples. *Rapid Commun. Mass Spectrom*. **2013**, *27*, 2472-2482; doi:10.1002/rcm.6704.

(47)   Hamme, R. C.; Emerson, S. R. Measurement of dissolved neon by isotope dilution using a quadrupole mass spectrometer. *Mar Chem*. **2004**, *91*, 53-64. doi:10.1016/j.marchem.2004.05.001.

(48)   Manning, C. C.; Stanley, R. H. R.; Lott, D. E. Continuous Measurements of Dissolved Ne, Ar, Kr, and Xe Ratios with a Field-Deployable Gas Equilibration Mass Spectrometer. *Anal. Chem*. **2016**, *88*(6), 3040-3048; doi:10.1021/acs.analchem.5b03102.

(49)   Becker, M. W.; Charbeneau, R. J. First-passage-time transfer functions for groundwater tracer tests conducted in radially convergent flow. *J. Contam. Hydrol*. **2000**, *40*(4), 299-310; doi:10.1016/S0169-7722(99)00061-3.

(50)   Becker, M. W.; Shapiro, A. M. Tracer transport in fractured crystalline rock: Evidence of nondiffusive breakthrough tailing. *Water Resour. Res*. **2000**, *36*(7), 1677-1686; doi:10.1029/2000WR900080.

(51)   Kang, P.; Le Borgne, T.; Dentz, M.; Bour, O.; Juanes, R. Impact of velocity correlation and distribution on transport in fractured media: Field evidence and theoretical model. *Water Resour. Res*. **2015**, *51*(2), 940-959; doi:10.1002/2014WR015799.

(52)   Gupta, S. K.; Stephen Lau, L.; Moravcik, P. S. Ground-Water Tracing with Injected Helium.

Ground Water **1994**, *32*(1), 96-102.

(53) Gupta, S. K.; Moravcik, P. S.; Stephen Lau, L. Use of Injected Helium as a Hydrological Tracer. *Hydrol. Sci. J*. **1994**, *39*(2), 109-119; doi:10.1080/02626669409492728.

(54) Sanford, W. E.; Shropshire, R. G.; Solomon, D. K. Dissolved gas tracers in groundwater: Simplified injection, sampling, and analysis. *Water Resour. Res*. **1996**, *32*(6), 1635-1642; doi:10.1029/96WR00599.

(55) Visser, A.; Singleton, M. J.; Esser, B. K. Xenon Tracer Test at Woodland Aquifer Storage and Recovery Well. *Lawrence Livermore Natl. Lab. Rep*. **2014**.

(56) Laidlaw, I. M. S.; Smart, P. L. An Evaluation of Some Fluorescent Dyes for Water Tracing. *Water Resour. Res*. **1977**, *13*(1), 15-33.

(57) Magal, E.; Weisbrod, N.; Yakirevich, A.; Yechieli, Y. The use of fluorescent dyes as tracers in highly saline groundwater. *J. Hydrol*. **2008**, *358*, 124-133; doi:10.1016/j.jhydrol.2008.05.035.

(58) Shakas, A.; Linde, N.; Baron, L.; Bochet, O.; Bour, O.; Le Borgne, T. Hydrogeophysical characterization of transport processes in fractured rock by combining push-pull and single-hole ground penetrating radar experiments. *Water Resour. Res*. **2016**, *52*(2), 938-953; doi:10.1002/2014WR015716.

(59) Uddin, M. K.; Dowd, J. F.; Wenner, D. B. Krypton Tracer Test to Characterize the Recharge of Highly Fractured Aquifer in Lawrenceville, Georgia. *Proc. Georg. Water Resour. Conf*. **1999**, 516-519.

(60) Le Borgne, T.; Bour, O.; Riley, M. S.; Gouze, P.; Pezard, P. A.; Belghoul, A.; Lods, G.; Le Provost, R.; Greswell, R. B.; Ellis, P. A.; Isakov, E.; Last, B. J. Comparison of alternative methodologies for identifying and characterizing preferential flow paths in heterogeneous aquifers. *J. Hydrol*. **2007**, *345*, 134-148; doi:10.1016/j.jhydrol.2007.07.007.

(61)   Labasque, T.; Aquilina, L.; Vergnaud, V.; Hochreutener, R.; Barbecot, F.; Casile, G. C. Inter-comparison exercises on dissolved gases for groundwater dating - (1) Goals of the exercise and site choice, validation of the sampling strategy. *Appl Geochemistry.* **2014**, *40*, 119-125; doi:10.1016/j.apgeochem.2013.11.007.

(62)   Sugisaki, R.; Taki, K. Simplified analyses of He, Ne, and Ar dissolved in natural waters. *Geochem J.* **1987**, *21*, 23-27.

(63)   Aeschbach-Hertig, W.; Peeters, F.; Beyerle, U.; Kipfer, R. Palaeotemperature reconstruction from noble gases in ground water taking into account equilibration with entrapped air. *Nature* **2000**, *405*(6790), 1040-1044.

(64)   Ayraud, V.; Aquilina, L.; Labasque, T.; Pauwels, H.; Molenat, J.; Pierson-Wickmann, A. C.; Durand, V.; Bour, O.; Tarits, C.; Le Corre, P.; Fourre, E.; Merot, P.; Davy, P. Compartmentalization of physical and chemical properties in hard-rock aquifers deduced from chemical and groundwater age analyses. *Appl. Geochem*. **2008**, *23*(9), 2686-2707; doi:10.1016/j.apgeochem.2008.06.001.